Vol. 337: 51–61, 2007 | MARINE ECOLOGY PROGRESS SERIES
Mar Ecol Prog Ser | Published May 14

Seasonal chlorophyll *a* fluxes between the coastal Pacific Ocean and San Francisco Bay

Maureen A. Martin[1,*], Jon P. Fram[2], Mark T. Stacey[1]

[1]Department of Civil Environmental Engineering, 750 Davis Hall, University of California, Berkeley, California 94720-1714, USA
[2]Marine Science Institute, Building 520, Room 4013, University of California, Santa Barbara, California 93106-6150, USA

ABSTRACT: We measured chlorophyll *a* (chl *a*) fluxes between San Francisco Bay and the coastal ocean for 2 d in March 2002, October and November 2002, and June 2003; 1 d during neap tide and 1 d during spring tide. We applied harmonic analysis to velocity and chl *a* data to model scalar and velocity fields during a spring–neap cycle. We then integrated these data over the fortnightly period to calculate net dispersive fluxes. The net flux consisted of an advective and dispersive component. Dispersive flux was decomposed into physical mechanisms such as tidal pumping, steady circulation and unsteady circulation. Net flux was large and directed out of San Francisco Bay during spring, large and into the estuary during summer, and effectively zero during fall surveys. The direction of advective flux was always out of the estuary and the magnitude depended on advective speed and mean chl *a* concentration. Dispersive flux was of a similar magnitude to advective flux each season and changed direction seasonally. Based on historical records and simultaneous observations, we conclude the reversal of the dispersive flux is most likely due to difference in phytoplankton growth conditions (or difference in timing of blooms) in the coastal ocean and estuary. During the spring, phytoplankton bloom in the estuary, creating a net seaward flux. In summer, during upwelling, phytoplankton bloom in the coastal ocean, driving a net flux into the estuary. Tidal pumping accounted for 79% of spring, 63% of fall and 93% of summer dispersive flux. Steady fluxes were about 1 order of magnitude smaller than tidal pumping, and unsteady fluxes yet another 1 order of magnitude smaller. The dominance of tidal pumping implies that seasonal variability of ocean–estuary exchange is set almost entirely by variation in the gradient of chl *a* concentrations between the ocean and the estuary such that the variability of ocean-estuary exchange is set by variation in the occurrence of estuarine and oceanic blooms.

KEY WORDS: Chlorophyll *a* physical transport · Phytoplankton ecology · San Francisco Bay · Statistical analysis

INTRODUCTION

San Francisco Bay is an urbanized estuary exchanging waters with the coastal Eastern Pacific Ocean. Biological exchange between ocean and estuary may be important to understanding how climate change will affect the San Francisco Bay ecosystem. Several studies have shown that abundance of organisms such as zooplankton, rockfish, and shorebirds corresponds to physical changes in the Pacific Ocean basin, such as changes in sea surface temperature (McGowan et al. 1998, 2003, Chavez et al. 2003). In addition to organism abundance, studies focused on the Pacific basin ecology have found that species composition changes (Chavez et al. 2003). Species shifts have also been observed in the phytoplankton community of San Francisco Bay around times coincident with Pacific basin shifts (Cloern & Dufford 2005). Quantifying phytoplankton exchange between San Francisco Bay and the coastal Pacific Ocean is a first step to understanding how changes in environmental conditions may propagate through the ecosystem.

*Email: maursm@berkeley.edu

Net ocean–estuary phytoplankton exchange is dependent on both physical and biological differences between ocean and estuary waters; the residual flux mechanisms outlined below combined with differences in species composition or differences in concentrations of phytoplankton create net exchange. In San Francisco Bay, as in many estuarine systems, tidal flows are the dominant forcing mechanism defining the velocity field. Vertical, lateral, and temporal variations in both the velocity and scalar fields define a complex, potentially 3-dimensional, flux field, which must be averaged over long timescales to define the residual scalar flux. Studies of estuarine salt fluxes (Fischer et al. 1979) have identified several dominant mechanisms that determine the residual flux of salt; below we review this work in the context of our study site.

Physical estuarine transport mechanisms: residual flux processes

Tidal pumping and trapping

When tidal flows interact with bathymetry, ebb–flood asymmetries develop in both the flow structures and the scalar concentrations. Stommel & Farmer (1952) described 'tidal pumping' as a jet that enters an embayment during the flood tide, and radial return flow during the ebb. The result is a net exchange of water, whereby some oceanic waters remain within the embayment after the ensuing ebb tide. A second transport mechanism that involves tidal interaction with bathymetry was analyzed extensively by Okubo (1973), and has become known as 'tidal trapping'. In this case, a residual flux is created by the relative phasing of cross-sectionally averaged tidal velocity and scalar concentration. If tidal currents and variations in scalar concentration are a quarter-cycle out of phase, then the net transport of the scalar by the tides would be zero due to the symmetry of flood and ebb tide concentrations. If this phasing is shifted slightly, such that, for example, flood tides have higher concentrations than ebbs, then a net flux of scalar is created that is directed into the estuary (reversed if ebbs have higher concentrations).

Our observations at the Golden Gate have established that both of these mechanisms are important for net scalar exchange, and they will collectively be referred to as tidal pumping henceforth. Tidal exchange processes are further modified at the Golden Gate by the formation of a headland eddy during the flooding tide on the north side of the channel (Fram et al. 2007). This eddy is retained in the shallow region between the primary tidal channel, Angel Island, and Point Covallo (Fig. 1). On the ensuing ebb tide, this eddy moves seaward, maintaining its distinct scalar character such that water that entered the estuary early on the flood tide exits early in the ebb, rather than late as would be expected in a symmetric tidal flow. In repect to salt, we determined that these 2 tidal exchange mechanisms combined contributed approximately 80% to the total residual salt flux (Fram et al. 2007).

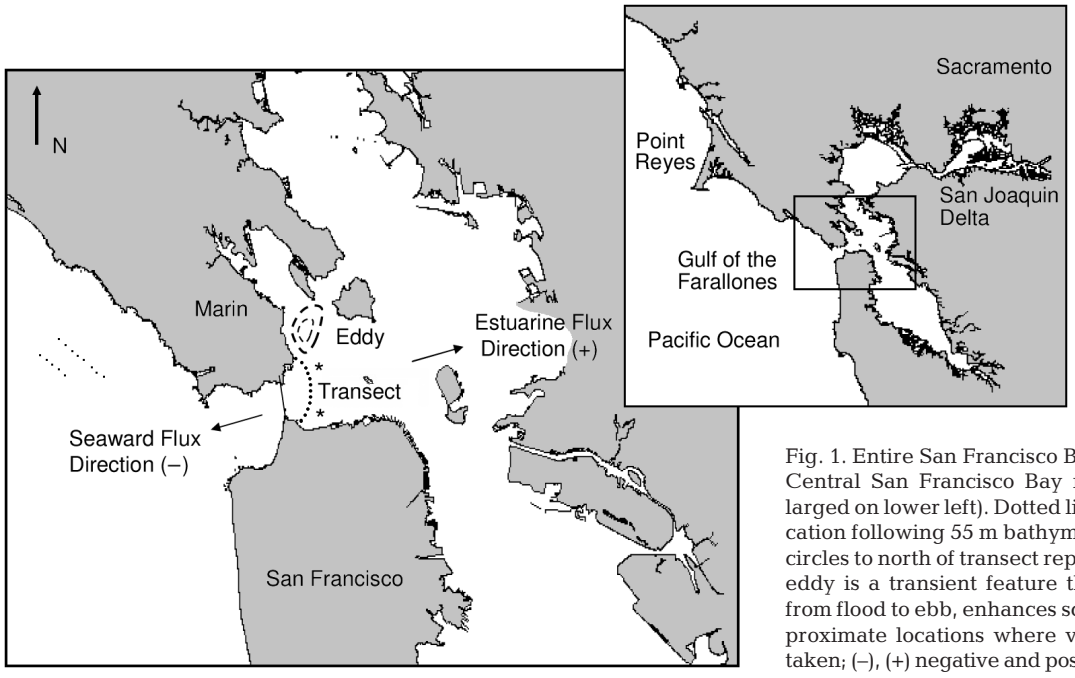

Fig. 1. Entire San Francisco Bay (upper right) with Central San Francisco Bay marked by box (enlarged on lower left). Dotted line shows transect location following 55 m bathymetry contour; dashed circles to north of transect represent eddy location; eddy is a transient feature that, when tide turns from flood to ebb, enhances scalar exchange. *: approximate locations where vertical profiles were taken; (–), (+) negative and positive flux respectively

Steady exchange flows

In addition to tidal forcing, a fundamental characteristic of estuaries is the density gradient defined by the freshwater–saltwater gradient. This gradient establishes a residual flow through a baroclinic pressure gradient (Hansen & Rattray 1965). Combined with a seaward barotropic pressure gradient, the net flow consists of a seaward surface flow and a landward bottom flow. The timing and magnitude of baroclinic exchange flows are influenced to a great extent by tidally-induced turbulent mixing, creating variability in the estuarine exchange at the spring–neap (Geyer et al. 2000, Ribeiro 2004) and even tidal (Stacey et al. 2001) timescales. The implication of this flow structure for net scalar fluxes depends on the vertical structure of the scalar. If the scalar is well-mixed vertically, the baroclinic scalar flux will be zero, with the upper and lower layer fluxes canceling each other. If, however, there is a vertical gradient in the scalar, then baroclinic exchange flows can create a net flux along the axis of the estuary. This is frequently invoked to explain the landward flux of salt that acts in opposition to seaward freshwater flow, but at the Golden Gate this flux mechanism only accounts for about 10% of the total salt flux (Fram et al. 2007).

The remainder of the salt flux at the Golden Gate was explained by a lateral steady exchange flow, where flow was directed into the estuary on the south and out of the estuary on the north side of the channel. Due to the geometry of San Francisco Bay and the fact that freshwater flow primarily enters through the northern reach of the bay, the north side of the Golden Gate channel was somewhat fresher than the south side. This asymmetry, combined with a steady exchange flow led to a net flux of salt into the bay (Fram et al. 2007).

Implications for phytoplankton transport

The physical processes described in the preceding section will create a net flux of phytoplankton, as long as phytoplankton gradients are established, either between the bay and the ocean (in the case of tidal exchange) or in the vertical and lateral directions within the bay (in the case of steady exchanges). These gradients, which vary over a wide range of spatial and temporal scales, are strongly influenced by both biological and physical processes. When the growth rate of phytoplankton exceeds transport and loss (respiration & predation) rates, blooms can occur. Typically blooms are characterized by isolated patches of high chlorophyll or phytoplankton concentration that are triggered by changes in the physical environment (Martin 2003). Strong spatial gradients of chlorophyll develop as a consequence of the inherent patchy distribution of phytoplankton during a bloom. In this particular study we did not seek to quantify which processes (light, grazing, nutrients etc.) are creating the spatial differences in chlorophyll concentrations; we were merely interested in the presence of spatial chlorophyll gradients and hence exchange induced by the physical mechanisms outlined above. The goal of this study was to quantify the net chlorophyll exchange between San Francisco Bay and the coastal Pacific Ocean over a neap–spring tidal cycle and to distinguish which physical processes are responsible. The resulting fluxes of chlorophyll are considered in a seasonal context.

MATERIALS AND METHODS

Field observations. To calculate net fluxes we measured cross-sectional velocity and scalar concentrations (salinity, chlorophyll and sediment) across the mouth of San Francisco Bay. The transect path was located just east of the Golden Gate bridge and followed a 55 m bathymetric contour (Fig. 1). This contour was chosen to avoid navigation hazards such as a bathymetric sill and the base of the Golden Gate Bridge. Data were collected during each of 3 seasons: spring runoff (March 6–7 and 13–14, 2002); fall relaxation (October 29 and November 6–7, 2002); and summer upwelling (June 3–4 and 10–11, 2003). During the summer and fall experiments, 12 min transects across the channel were repeated continuously for 25 h for 2 d; 1 d during spring tide and 1 d during neap tide. Because of inadequate navigation equipment, overnight work was not possible during the first winter/spring experiment, so data was collected only during daylight hours.

Velocity and scalar concentrations were measured aboard the USGS RV 'Turning Tide'. Velocity was measured by a boat-mounted 300 kHz acoustic Doppler profiler (RDI ADCP), which was configured to have 1 m vertical resolution. Scalar concentrations were obtained from an undulating towed vehicle (Sea-Sciences Acrobat) as well as a boat-mounted CTD (RBR). The tow-yo package included instruments measuring temperature, salinity, depth (SeaBird), optical backscatter (D&A OBS), and UVA chlorophyll fluorescence (Turner SCUFA) and photosynthetic radiation (Licor PAR). The tow body was only able to fly reliably from a depth of about 10 m to about 50 m.

During each experiment vertical profiles were taken at the southern and northern ends of the transect during flood, ebb and slack tide. Profiles measured salinity, temperature, fluorescence and turbidity. During

each of these profiles, water samples were collected at 3 different depths (approximately 10, 30, and 55 m) for calibrating optical instruments. To calibrate the fluorometer, sample water was filtered and chlorophyll *a* (chl *a*) was extracted following EPA method 445.0. High surface irradiance and turbidity were not accounted for in the fluorometer calibration.

Data analysis. Current and scalar fields were mapped on to a 2D arcing grid with 50 m wide × 1 m deep cells. The grid is arced instead of flat to follow the boat track and is roughly perpendicular to the primary tidal flow direction. Raw scalar data were interpolated within the area where the tow-yo body was able to fly (10 to 50 m depth) using ordinary kriging (Fram et al. 2007). Kriged data from that area were then extrapolated to the surface and bottom boundaries using empirical equations fitted to the vertical profiles collected during flood, ebb and slack tide in fall and summer. The empirical equation used to interpolate data to the top and bottom boundaries was chl $a\,(z) = a_1 + a_2 \exp(-a_3 z)$, where z is the depth below the surface. The unknown parameters (a_1, a_2, a_3) are fit for each column of the data grid. This functional form was not chosen for mechanistic or biological reasons but was merely the best fit for the profiles observed. One of the features of the data that is reflected by this functional fit is a trend towards higher concentrations at depth than at the surface. This vertical distribution of chl *a* was observed during fall and summer, but because we did not have sufficient instruments during the spring, it is not known if this functional form accurately describes vertical distribution during spring.

To calculate net fluxes between the ocean and estuary, an integration over time of the observed velocity (U) and chlorophyll (C) was required (Eq. 1):

$$\text{Net flux} = \frac{1}{T}\int_0^T\int_0^Z\int_0^Y UC\,\partial y\,\partial z\,\partial t \quad (1)$$

where t = time; T = the 2 wk period over which the flux is integrated; Y (north–south) and Z (up–down) represent the cross-sectional area through which the flux passes, or perpendicular to the flux direction.

For purposes of discussion, we considered the net exchange of a scalar to be the mass exchange rate on timescales longer than the tidal and fortnightly (spring–neap) timescales. Due to subtle tidal asymmetries, and the non-uniform nature of the data, a straight temporal average of the observations would not adequately resolve the sub-tidal fluxes. Instead, we relied on the integration of harmonics using the known tidal frequencies (ω) (K1: 24 h period, M2: 12.42 h, S2: 12 h, N2: 12.66 h, O1: 25.8 h, and M4: 6.21 h). In this analysis, the observed velocity and chlorophyll for each grid cell are fit with an amplitude, A_i, and phase, ϕ_i, for each tidal frequency (or harmonic). The result is a time series for velocity and concentration at each point in the cross-section that can be directly integrated to define a net flux:

$$u(t) = \sum A_i^u \times \sin(\omega_i t + \phi_i^u) \qquad c(t) = \sum A_i^c \times \sin(\omega_i t + \phi_i^c) \quad (2)$$

This analysis was applied to salinity with excellent fitting results (R^2 = ~0.98; Fram et al. 2007). The quality of fit for chlorophyll, however, is reduced due to the inherent variability in biological scalars. Cross-sectional average fits for summer and spring surveys were $R^2 = 0.79$ and for fall survey $R^2 = 0.83$. Between 40 and 50 points were typically averaged over to calculate the cross-sectional average. For illustrative purposes we show the harmonic fit for the cross-sectional average for summer, when calculating the fluxes, however, each grid cell has a harmonic fit (Fig. 2).

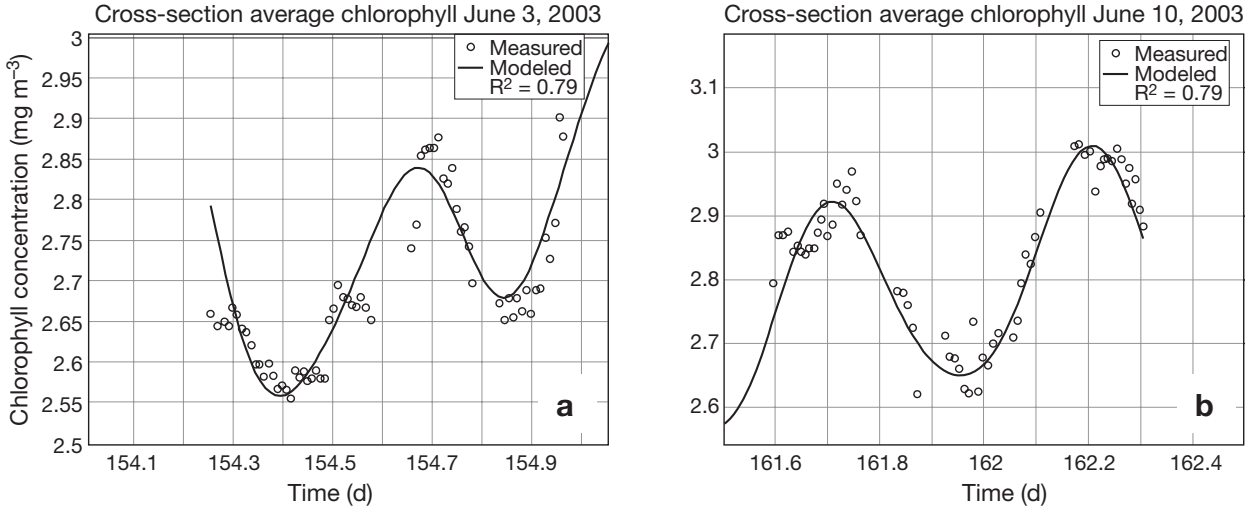

Fig. 2. Example of harmonic fit for cross-sectional average chl *a* in summer data set. (○) Actual data collected; curve: harmonic fit. R^2 for fitting both (a) June 3 and (b) June 10 is 0.79. For flux calculations, harmonics were fitted for each grid cell

To discern which physical processes governed the net flux we decomposed the velocity and scalar time-series following Fischer (1972). The velocity and scalar time series were broken down into average and fluctuating components. The components of the velocity breakdown are u_0: a temporal and spatial average; u_1: a cross-sectional average with temporal variability; u_2: the tidal cycle average; and u_3: a cross-sectional deviation (Fig. 3). The same analysis was applied to chl *a*.

We applied this decomposition to each of the seasonal data sets to separate and quantify the physical processes responsible for the dispersive flux of chlorophyll. To define the cross-sectionally averaged mean outflow (u_0) or the advective component, we could not rely solely on the harmonic fitting, due to its small magnitude. Instead, we applied a Bay-scale freshwater mass balance (Fram et al. 2007):

$$Q_f = u_0 \times A_1 = Q_{delta} + Q_{localrivers} + Q_{mud} - A_2\left(\frac{\partial Elevation}{\partial t} + Evaporation\right) \quad (3)$$

where Q_f is the freshwater flow through the Golden Gate and is equal to the temporal and spatial average of velocity, u_0, multiplied by the cross-sectional area over which fluxes were measured, A_1. Flow from the Sacramento/San Joaquin delta is Q_{delta}, flow from local rivers such as Coyote Creek are $Q_{localrivers}$, flow from municipal waste discharge is Q_{mud}, and the last term is evaporation that is multiplied by the surface area of the Bay, A_2.

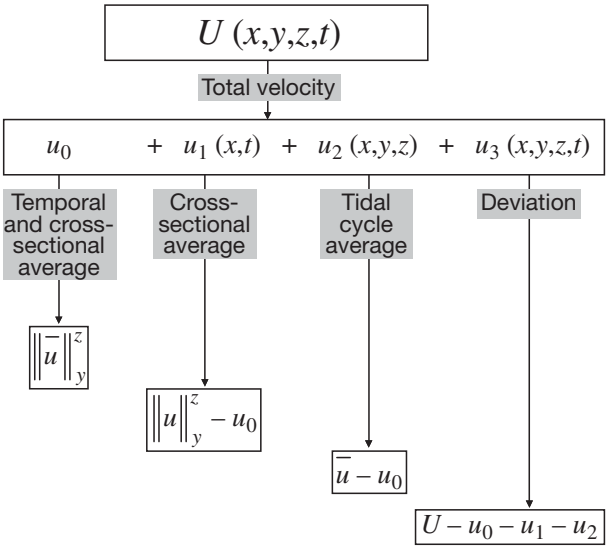

Fig. 3. Velocity field decomposed into average and fluctuating components. *x*-direction is longitudinal or along axis of estuary, *z*-direction is vertical, and *y*-direction lateral. First term (u_0) is cross-sectional (vertical bars) and temporal (overbar) average over tidal cycle; second term (u_1) is cross-sectional average, retaining variability in *x* and *t*; third term (u_2) is temporal average minus mean, retaining variability in all spatial dimensions; fourth term (u_3) is velocity remaining after subtraction of previous terms from original velocity

The flux of chl *a* into or out of Central San Francisco Bay through the cross-section of the Golden Gate is described by:

$$\text{Flux} = M = Q_f C_0 + A_1\left[\overline{u_1 c_1} + \|u_2 c_2\|_y^z + \overline{\|u_3 c_3\|_y^z}\right] \quad (4)$$

River advection | Tidal pumping + trapping | Steady circulation | Unsteady shear flow

The first term on the right-hand side of the equation represents the transport of the mean chlorophyll concentration by the river outflow, where Q_f is freshwater flow as defined above ($m^3\ s^{-1}$) and C_0 is the cross-sectionally and temporally averaged concentration ($mg\ m^{-3}$), which we will refer to as the advective flux. The remaining terms represent dispersive processes, where A_1 is cross-sectional area of our study site (m^2). The time average of u_1c_1 is the flux due to tidal cycle correlation of the cross-sectional averages and, for our study site, is considered to be the net effect of both tidal pumping and trapping. The cross-sectional average of u_2c_2 is the flux due to steady circulation and is created by both baroclinic forcing and time-variable stratification events. The spatial and temporal average of u_3c_3 is the unsteady net flux due to oscillating shear flow and includes mechanisms on smaller time scales.

There are 2 possible ways to apply Fischer's analysis to non-rectangular grids. The first involves averaging vertically initially, and the second involves averaging laterally initially. While the 2 averaging techniques provide slightly different results, the difference between them is less than the uncertainties in our estimates. As a result, we present an average of the results from the 2 methods.

Sensitivity analysis. To test how sensitive each of the flux mechanisms is to changes in the harmonics we recalculated the fluxes using harmonic values that correspond to a fit 0.1 less than the optimum fit. In other words, if the optimized harmonics had an R^2 value of 0.90 we established the parameter range over which the R^2 remained above 0.80. The minimum and maximum values that were within the specified R^2 range were used to recalculate the fluxes. Error bars were constructed for each flux component based on the largest and smallest recalculated results.

RESULTS

The direction of the net flux is determined by the magnitude and direction of both the dispersive and advective component. The direction of the advective component is always out of the estuary (seaward) and

the direction of the dispersive component changes seasonally. During the spring and fall surveys, the direction of the total dispersive flux was out of the estuary whereas during the summer survey it was into the estuary. Thus, the net flux of chlorophyll was out of the estuary during the spring and fall experiments, but the dispersive flux into the estuary was sufficiently large during summer to reverse the net flux into the estuary (Table 1, Fig. 4).

Advection

The advective flux was largest during the spring experiment because freshwater flow and mean chl *a* concentration were greatest (Table 2). Freshwater flows were lowest during the fall and estuarine chlorophyll concentrations were also low, yielding the smallest advective flux. Freshwater flows were unusually high during this summer study leading to a relatively large advective flux. During a more typical summer, freshwater input would probably be lower and the advective flux smaller.

Dispersion

The direction of the net dispersive flux was out of the estuary during the spring surveys and into the estuary during the summer surveys (Table 1). During the fall, the dispersive flux was relatively small, and within the uncertainty of the estimate of zero (Fig. 4). Below we discuss the mechanisms that cause this seasonal pattern; the separation of the fluxes into mechanisms is based on the terms in Eq. (4).

Table 1. Net chl *a* flux (mg chl *a* s^{-1}) for spring, fall and summer surveys. Negative values indicate flux is out of estuary

	Spring (2002)	Fall (2002)	Summer (2003)
Advection	−1858	−287	−1121
Total dispersion	−5860	−465	2406
Net flux	−7718	−752	1285

Table 2. Advective flow rates and mean chl *a* concentration calculated for Central San Francisco Bay

Parameter	Spring (2002)	Fall (2002)	Summer (2003)
Freshwater flow Q_f (m^3 s^{-1})	−613	−139	−406
Mean chl *a* concentration C_0 (mg m^{-3})	3.03	2.06	2.76

Tidal pumping

Tidal pumping was the dominant flux mechanism in all surveys and accounted for 79% of net dispersive flux during spring, 64% during fall, and 93% during summer. The spring and fall tidal pumping fluxes were 5262 and 327 mg s^{-1} respectively out of the estuary (Table 3). Summer tidal pumping flux was 2112 mg s^{-1} into the estuary. These flux results indicate that flood and ebb waters have different chlorophyll concentrations and there is a phase difference between the timing of slack water and the maximum chlorophyll concentration. At our site, Fram et al. (2007) found that the phase shift between velocity and salinity concentration varied seasonally due to baroclinic forcing of the headland eddy described above. The result is an increase in tidal pumping flux during winter/spring conditions

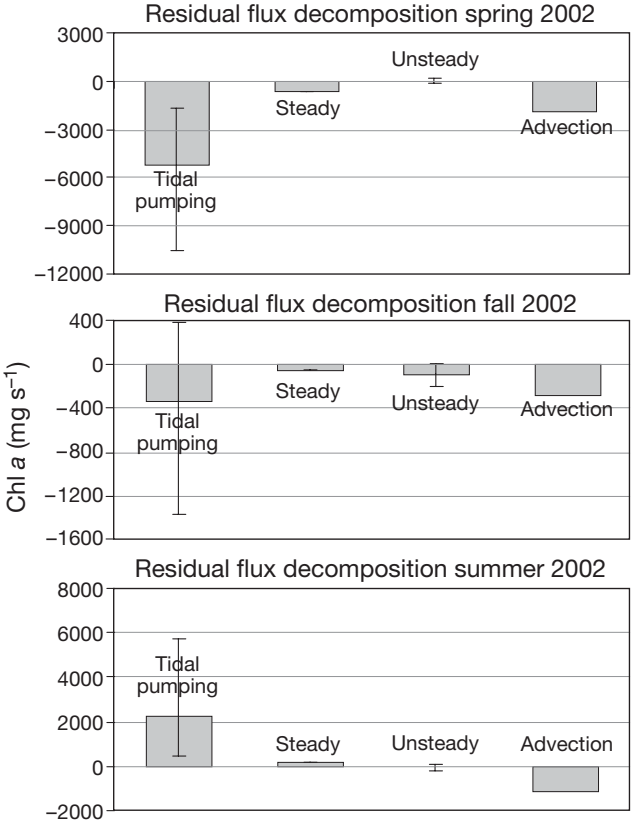

Fig. 4. Seasonal magnitude and direction of residual flux components in Central San Francisco Bay. Negative values indicate flux out of estuary, positive values flux into estuary. Error bars on dispersive components were calculated by testing sensitivity of harmonics. Advective fluxes do not have error bars because they were not calculated using harmonic analysis

Table 3. Seasonal dispersive chlorophyll fluxes (mg s^{-1}) separated into physical processes

Process	Spring (2002)	Fall (2002)	Summer (2003)
Tidal pumping	−5262	−327	2291
Steady	−618	−44	139
Unsteady	20	−94	−24

relative to fall. Although this trend is consistent with the chlorophyll fluxes measured (Table 3), the magnitude of the seasonal change in chlorophyll fluxes exceeds what would be expected from this purely physical mechanism. As a result, we conclude that the seasonal trends in chlorophyll fluxes, particularly the reversal of the flux direction in the summer, must be driven by changes in the ambient chlorophyll gradient. This topic will be discussed in more detail in subsequent sections.

Steady circulation

Steady circulation fluxes were about 1 order of magnitude smaller than tidal pumping fluxes during spring and comprised a vertical and lateral component. During spring and fall, steady fluxes were 618 and 44 mg s^{-1} out of the estuary respectively, and during the summer 139 mg s^{-1} into the estuary. A steady flux direction is determined by the chlorophyll distribution relative to the density induced circulation.

Unsteady shear flow

Fluxes due to unsteady shear flow were 1 order of magnitude smaller than steady fluxes during spring and summer and very sensitive to changes in harmonics. During fall, unsteady flux was of a similar magnitude to steady flux, but was much more sensitive. This being so, we will not further discuss the mechanisms or implications of these fluxes.

Sensitivity and error analysis

Although tidal pumping is the most sensitive of the flux mechanisms to changes in M2 amplitude and phase, the direction of the tidal pumping flux during spring and summer did not change. The magnitude of the flux could be up to 100% larger in spring and 150% in summer than the reported optimized values (Fig. 4). The fall tidal pumping flux was very sensitive to small changes in the harmonics. Fall flux direction was unclear and the magnitude could be up to 4000% more or less than the optimized value, and we conclude that this result did not differ significantly from zero.

Because of the incomplete tidal cycle coverage during the spring, harmonics with periods longer than 24 h could not be effectively constrained. The K1 phase harmonic was poorly constrained and a phase between 0 and π yielded an equally good fit (R^2) as a phase between 0 and –π. The K1 phase primarily affects mean chlorophyll concentration C_0 and the steady flux; the ambiguity between positive and negative phases lead us to conclude that the steady flux estimate during the spring season was not significantly different from zero. This fact does not undermine the conclusion that the net dispersive flux is out of the estuary during the spring season, however, since it is dominated by tidal pumping and is strongly dependent on M2 harmonics.

DISCUSSION

Although we only collected data for several days during each season for 1 yr, the results are in agreement with descriptions in previous studies of seasonal patterns of circulation and chlorophyll distribution (Cloern 1996, Pennington & Chavez 2000). The direction of the advective or river component was always out of the estuary, i.e. seaward. River inputs to the estuary are greatest during the spring when the snow pack begins to melt, and these correspond to the largest advective velocities out of the estuary and largest advective flux (Conomos et al. 1979). The direction of the dispersive component, which is comparable to or greater than the advective flux, changes seasonally. During the spring and fall the direction of the total dispersive flux is out of the estuary whereas during the summer it is into the estuary. The direction of dispersive transport changes seasonally because the distribution of chlorophyll changes seasonally.

Dispersive flux can be described by $\text{Flux} = -K_x \frac{\partial C}{\partial x}$ where K_x is the dispersion coefficient and $\frac{\partial C}{\partial x}$ is the spatial gradient of chlorophyll along the direction of the major flow axis, primarily east–west at our field location. The dispersion coefficient does not change signs across seasons (for more discussion see Fram et al. 2007) so the net ocean–estuary exchange is set by the chlorophyll gradient. To evaluate the change in the chlorophyll gradient across the ocean–estuary interface by season, we consider our chlorophyll measurements in the context of the temperature and salinity of the associated water mass. In Fig. 5, we present spring, fall and summer observations of temperature and salinity, with color-coded chlorophyll measurements. In Fig. 5, oceanic waters are on the lower right (high

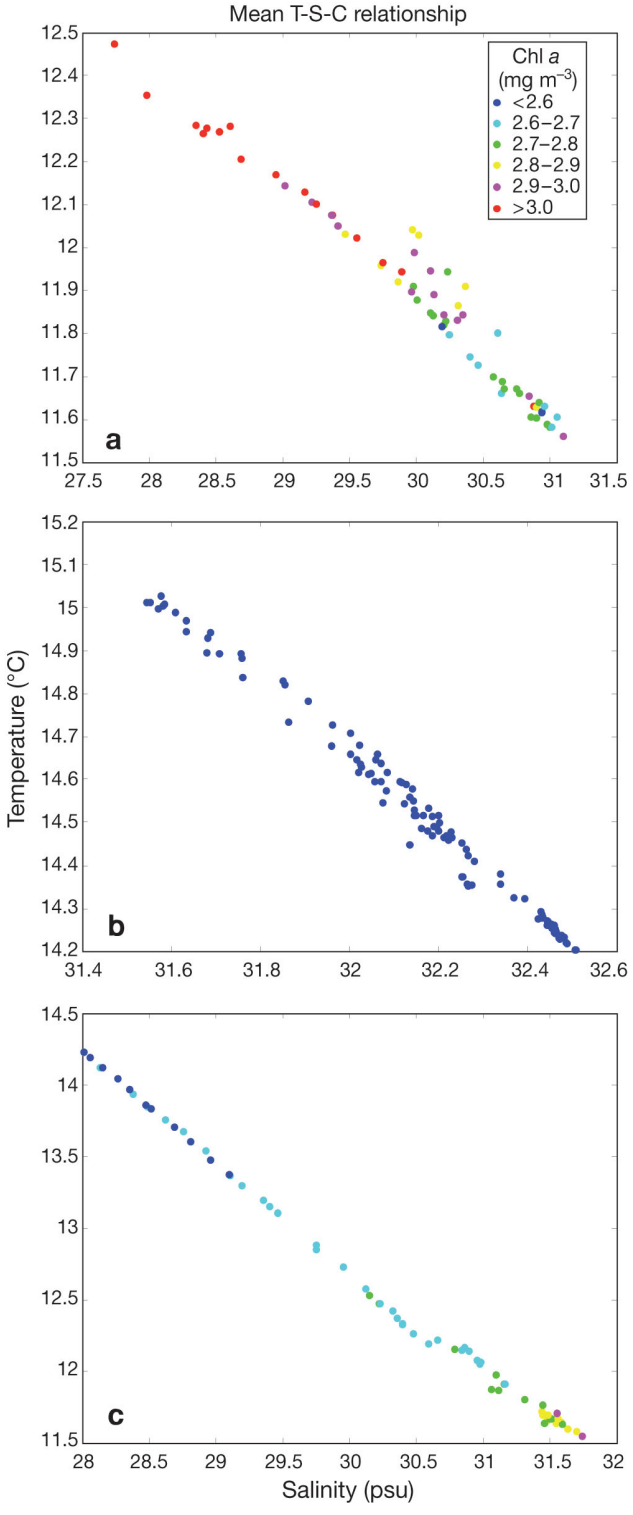

Fig. 5. (a) Spring, (b) fall, and (c) summer temperature (T), salinity (S) and chl *a* (C) measurements in San Francisco Bay. Estuary water signature is low salinity–high temperature, and coastal water signature high salinity–low temperature. Colors indicate concentrations of chlorophyll (mg m^{-3}). Chl *a* concentration is higher in estuary waters during spring, uniform during fall, and higher in coastal waters during summer, illustrating that chlorophyll source and gradient change seasonally

salinity, low temperature), and estuarine waters on the upper left (low salinity, high temperature) of each graph. During spring (Fig. 5a), high concentrations of chlorophyll were associated with estuarine waters. During the summer (Fig. 5c), this gradient was reversed, and the highest chlorophyll concentrations were associated with oceanic waters.

Combining these results with a relatively constant tidal dispersion coefficient, we conclude that during the spring the dispersive flux of chl *a* is out of the estuary, due to a positive concentration gradient, i.e. higher in the estuary and lower in the coastal ocean. During summer the gradient is reversed, with higher concentrations in the coastal ocean and lower concentrations in the estuary, so the dispersive flux is into the estuary. During our fall survey there was essentially no chl *a* gradient and the dispersive flux was close to zero. The variation in ocean-estuary chlorophyll gradient and hence exchange therefore depends on the seasonal variation of phytoplankton net growth conditions in both the estuary and coastal environments.

Seasonal variability in estuarine phytoplankton growth

There are distinct seasonal phytoplankton cycles within San Francisco Bay. North San Francisco Bay historically had blooms during the summer, but these have declined since 1989 when an invasive clam was introduced to the ecosystem (Cloern 1996). Currently, the largest annual production of phytoplankton occurs during spring after the annual freshwater pulse reaches South San Francisco Bay. Freshwater flows are usually greatest between January and March. During neap tides, when mixing energy is low, this freshwater pulse stratifies the water column in parts of the estuary. When the water column is stratified, phytoplankton in the photic zone are decoupled from the benthos thereby reducing benthic grazing and exposure to tidally re-suspended sediments. Release from light and grazing-induced limitations leads to a bloom (Cloern 1982, 1991). The result is high concentrations of chl *a* within the estuary, especially in South San Francisco Bay, every spring.

Based on an earlier analysis of temperature and salinity (Fram et al. 2007), we found the water at the southern end of our transect was largely made up of South Bay waters. Although we do not have simultaneous measurements of conditions in South Bay, a bloom was likely occurring due to the coincidence of a peak freshwater pulse and neap tides during our spring surveys. During the spring of 2002, the Sacramento/San Joaquin River peak flow was on January 6 and, assuming that the travel time of the freshwater pulse from the Delta to South Bay is between 35 and 50 d (Uncles &

Peterson 1996), we would expect the pulse to arrive between February 10 and 26. Spring to neap tide transition occurred between February 27 and March 6 and it is reasonable to assume that this was the window within which the onset of a bloom occurred. Our measurements in Central Bay were made on March 6 and 7 and on March 13 and 14; therefore if the high concentration of estuarine chlorophyll measured during our spring surveys derived from a South Bay bloom, the travel time between Central and South Bay would be approximately 1 to 2 wk.

Although we cannot refine this description further with the data available at this point, we conclude that the direction of ocean–estuary exchange is gradient driven and will consistently be out of the estuary while there are estuarine blooms within the realm of Central exchange. The magnitude of phytoplankton exchange will depend on the intensity and duration of the bloom.

Seasonal variability in coastal phytoplankton dynamics

The normal pattern of coastal upwelling (typical in years without El Niño or La Niña conditions) on the west coast of the USA is driven by southerly winds and Ekman transport of surface waters offshore (Hickey 1979). This upwelling brings nutrients into the photic zone, releasing coastal phytoplankton from nutrient limitation in the photic zone (Hutchings et al. 1995). Generally, upwelling results in blooms of coastal phytoplankton. In Monterey Bay, increases in surface nitrate are observed initially after upwelling and high surface chlorophyll concentrations generally lag behind surface nitrate concentration by weeks (Pennington & Chavez 2000, Collins et al. 2003). During El Niño years, temperatures are warmer, the thermocline is deeper and waters in the photic zone tend to be low in nutrients. The opposite is true during La Niña when surface waters are cool, the thermocline is elevated, and surface nutrients from upwelled waters is greater than normal. These conditions lead to unseasonably low phytoplankton concentrations during El Niño and high concentrations during La Niña (Chavez et al. 2002). The period from January 2003 until spring 2004 was a 'normal' oceanic year, so our summer observations characterize normal conditions (Goericke et al. 2004).

During our summer observations, coastal chlorophyll concentrations were elevated compared to estuarine concentrations (http://sfbay.wr.usgs.gov/access/wqdata). National Marine Fisheries Service (NMFS) collected hydrographic and biological data (including chlorophyll concentration) from June 3 to 10 in the coastal region offshore from San Francisco. Their data indicates high surface chlorophyll concentrations (~25 mg m^{-3}) throughout their study, especially on June 10 to the north of San Francisco Bay (K. Sakuma, NMFS, pers. comm.). These blooms were most likely initiated by upwelling. Large (daily average >100 t s^{-1} 100 m^{-1} of coastline) offshore Ekman transport began on May 5, 2003 and, with the exception of June 3 to 6, continued until June 26 (www.pfeg.noaa.gov/products/PFEL). The break in the winds between June 3 and 6 may have initiated the very high chlorophyll concentrations measured by NMFS. Pennington & Chavez (2000) and Hutchings et al. (1995) found that diatoms, the dominant type of coastal phytoplankton (Chavez et al. 1991, Venrick 2002, Collins et al. 2003), bloom after large upwelling events during times of relatively low mixing. These data confirm that wind-driven upwelling initiated blooms in the coastal ocean offshore of San Francisco Bay during our study.

Coastal blooms during the summer result in a gradient-driven dispersive flux into the estuary. Our flux measurements from summer of 2003 are expected to be representative of summer conditions in most years, with the possible exception of El Niño years when the coastal bloom may be weakened or absent.

Implications for ocean–estuary exchange

The difference in timing of blooms in the estuary and coastal ocean establishes the annual cycle in net chlorophyll fluxes presented in Table 1. As conditions improve in the estuary during winter/spring neap tides, the net flux of chlorophyll is out of the estuary due to both advection and dispersive mechanisms. During the summer months, as estuarine chlorophyll concentration decreases and coastal upwelling begins, the ocean–estuary gradient of chlorophyll reverses, and the flux of chlorophyll is into the estuary. It is important to note that the shift in the direction of chlorophyll flux is not a function of different physical flux mechanisms, but rather purely a result of a changing gradient in chl *a*. Instead, the physical mechanism that dominates ocean–estuary exchange, tidal pumping, is relatively constant throughout the year, and will always create a down-gradient flux.

The transport rates calculated are large, the dispersive fluxes are gradient driven and chlorophyll gradients can change on timescales ranging from days to weeks. Although the gradient may be very large between the ocean and estuary, especially during the spring bloom and coastal upwelling, the net flux is ultimately limited by the balance between transport and growth timescales. The longer the bloom lasts, and the closer it is to the mouth of the estuary, the greater the amount of phytoplankton transported between coastal and estuarine ecosystems.

CONCLUSION

We calculated seasonal net fluxes of chl *a* at the Golden Gate Bridge using field measurements and harmonic analysis from March 2002, October and November 2002 and June 2003. Net chlorophyll fluxes were into the estuary during summer and seaward during fall and spring. The net flux consists of an advective and dispersive component. Advection is due to freshwater flow and therefore the magnitude of the advective flux is proportional to flow rate and the direction is always out of the estuary. Dispersive fluxes were broken down into several different physical mechanisms, tidal pumping, steady circulation and unsteady shear flow. Tidal pumping, which depends on different concentrations of chlorophyll between ebb and flood tide and timing asymmetries between tidal velocity and concentration maxima, was the dominant dispersive process contributing to net exchange year round.

The dispersive flux is gradient driven and changes direction seasonally based on the timing and magnitude of blooms in the coastal ocean and estuary. During the summer when coastal upwelling occurs, chlorophyll concentration is higher in the ocean than in the estuary, creating a gradient driven dispersive flux of coastal phytoplankton into the estuary. The opposite is true during spring when estuarine concentration is higher and there is a dispersive flux out of the estuary. During fall in our study, there were relatively low gradients and the direction and magnitude of transport could not satisfactorily be distinguished from zero. While the magnitude and timing of these fluxes may change annually or inter-annually, depending on the specific physical and biological conditions, the seasonal direction of chlorophyll fluxes measured in this study are consistent with physical and biological processes of a typical year.

Qualitatively similar results have been reported for several other estuaries along the western USA. Roegner & Shanks (2001) found that chlorophyll was transported from the coastal Pacific into South Slough, Oregon, during upwelling events. While there were no quantitative measurements made of the net flux, there was a relatively strong ocean–estuary gradient, suggesting that similar physical mechanisms (tidal pumping) may be controlling ocean–estuary exchange. In Willapa Bay, Washington, Newton & Horner (2003) found that the highest primary productivity in the bay was associated with the transport of coastally derived phytoplankton into the bay. This seasonal reversal of the ocean–estuary chlorophyll gradient may hold true for estuaries and embayments along eastern boundary currents where upwelling occurs, such as in Saldanha Bay in South Africa, and embayments along the NW Iberian coast.

In general, this type of analysis can be a useful tool for quantifying ocean–estuary chlorophyll exchange. This detailed mechanistic approach shows that, in Central San Francisco Bay, tidal dispersion dominates the transport of chlorophyll, which is a gradient driven process. However, the field data collection was fairly intensive and makes this type of analysis difficult to apply in many places. Future work should focus on relating the timescale of the chlorophyll gradient to the transport timescale, since the total transport into and out of a dispersion dominated estuary depends on how long the specific chlorophyll gradient persists. Few if any studies have investigated the timing, frequency and mechanisms reversing the ocean–estuary chlorophyll gradient. Considering such phenomenon in a seasonal and inter-annual context may provide more insight into how climate or anthropogenic changes will affect the primary productivity of similar coastal bays and estuaries. Specifically in San Francisco Bay, future work would greatly benefit from the routine measurement of water quality parameters in the adjacent coastal waters.

Acknowledgements. The work described in this paper was made possible with the crew of the USGS RV 'Turning Tide', captained by J. Cuetara, and operated with J. Yokomizo, C. Smith, and C. Battenfield. Field support was provided by D. Ralston, J. Grey, S. Talke, D. Sereno. This research was funded by California SeaGrant, #R/CZ-170 to M.T.S and T. Powell and by NSF, #OCE-0094317 to M.T.S.

LITERATURE CITED

Chavez FP, Barber RT, Kosro PM, Huyer A, Ramp SR, Stanton TP, Mendiola BR (1991) Horizontal transport and the distribution of nutrients in the coastal transition zone off Northern California: effects on primary production, phytoplankton biomass and species composition. J Geophys Res C 96:14833–14848

Chavez FP, Pennington JT, Castro CG, Ryan JP and 6 others (2002) Biological and chemical consequences of the 1997–1998 El Niño in central California waters. Prog Oceanogr 54:205–232

Chavez FP, Ryan J, Lluch-Cota SE, Niquen M (2003) From anchovies to sardines and back: multidecadal change in the Pacific Ocean. Science 299:217–221

Cloern JE (1982) Does the benthos control biomass in South San Francisco Bay? Mar Ecol Prog Ser 9:191–202

Cloern JE (1991) Tidal stirring and phytoplankton bloom dynamics in an estuary. J Mar Res 49:203–221

Cloern JE (1996) Phytoplankton bloom dynamics in coastal ecosystems: a review with some general lessons from sustained investigation of San Francisco Bay, California. Rev Geophys 34:127–168

Cloern JE, Dufford R (2005) Phytoplankton community ecology: principles applied in San Francisco Bay. Mar Ecol Prog Ser 285:11–28

Collins CA, Pennington JT, Castro CG, Rago TA, Chavez FP (2003) The California Current system off Monterey, California: physical and biological coupling. Deep-Sea Res II 50:2389–2404

Conomos TJ, Leviton AE, Berson M (eds) (1979) San Francisco Bay: the urbanized estuary: investigations into the natural history of San Francisco Bay and Delta with reference to the influence of man: 58th annual meeting of the Pacific Division/American Association for the Advancement of Science held at San Francisco State University, San Francisco, California, June 12–16, 1977. American Association for the Advancement of Science, Pacific Division, San Francisco, CA, p 47–84

Fischer HB (1972) Mass transport mechanisms in partially stratified estuaries. J Fluid Mech 53:671–687

Fischer HB, Brooks NH, Imberger J, Koh RCY, List EJ (1979) Mixing in inland and coastal waters. Academic Press, New York

Fram J, Martin M, Stacey M (2007) Residual flow creation: dispersive fluxes. J Phys Oceanogr (in press)

Geyer WR, Trowbridge JH, Bowen MM (2000) The dynamics of a partially mixed estuary. J Phys Oceanogr 30: 2035–2047

Goericke R, Venrick E, Mantyla A, Bograd SJ and 11 others (2004) The state of the California Current, 2003–2004: a rare 'normal' year. Calif Coop Ocean Fish Investig Rep 45:27–59

Hansen DV, Rattray M (1965) Gravitational circulation in straits and estuaries. J Mar Res 5:485–496

Hickey BM (1979) The California Current System—hypotheses and facts. Prog Oceanogr 8:191–279

Hutchings L, Pitcher GC, Probyn TA, Bailey GW (1995) The chemical and biological consequences of coastal upwelling. Wiley, New York

Martin AP (2003) Phytoplankton patchiness: the role of lateral stirring and mixing. Prog Oceanogr 57:125–174

McGowan JA, Cayan DR, Dorman LM (1998) Climate–ocean variability and escosystem response in the Northeast Pacific. Science 281:210–271

McGowan JA, Bograd SJ, Lynn RJ, Miller AJ (2003) The biological response to the 1977 regime shift in the California Current. Deep-Sea Res II 50:2567–2582

Newton JA, Horner RA (2003) Use of phytoplankton species indicators to track the origin of phytoplankton blooms in Willapa Bay, Washington. Estuaries 26:1071–1078

Okubo A (1973) Effect of shoreline irregularities on streamwise dispersion in estuaries and other embayments. Neth J Sea Res 6:213–224

Pennington JT, Chavez FP (2000) Seasonal fluctuations of temperature, salinity, nitrate, chlorophyll and primary production at station H3/M1 over 1989–1996 in Monterey Bay, California. Deep-Sea Res II 47:947–973

Ribeiro CHA, Waniek JJ, Sharples J (2004) Observations of the spring–neap modulation of the gravitational circulation in a partially mixed estuary. Ocean Dyn 54: 299–306

Roegner GC, Shanks AL (2001) Import of coastally-derived chlorophyll *a* to South Slough, Oregon. Estuaries 24: 244–256

Stacey MT, Burau JR, Monismith SG (2001) Creation of residual flows in a partially stratified estuary. J Geophys Res C 106:17013–17037

Stommel H, Farmer HG (1952) On the nature of estuarine circulation. Woods Hole Oceanographic Institute, Woods Hole, MA

Uncles RJ, Peterson DH (1996) The long-term salinity field in San Francisco Bay. Contin Shelf Res 16:2005–2039

Venrick EL (2002) Floral patterns in the California current system off southern California: 1990–1996. J Mar Res 60: 171–189

Editorial responsibility: Howard Browman (Associate Editor-in-Chief), Storebø, Norway

Submitted: March 23, 2006; Accepted: September 14, 2006
Proofs received from author(s): April 26, 2007